Antenna Effect in Noble Metal-Free Dye-Sensitized Photocatalytic Systems Enhances CO 2 -to-CO Conversion

Vasilis Nikolaou, Chinju Govind, Evangelos Balanikas, Jaya Bharti, Stéphane Diring, Eric Vauthey, Marc Robert, Fabrice Odobel

How to cite: Angew. Chem. Int. Ed. 2024, e202318299
doi.org/10.1002/anie.202318299

VIP CO_2 Reduction Very Important Paper

Antenna Effect in Noble Metal-Free Dye-Sensitized Photocatalytic Systems Enhances CO_2-to-CO Conversion

Vasilis Nikolaou, Chinju Govind, Evangelos Balanikas, Jaya Bharti, Stéphane Diring, Eric Vauthey,* Marc Robert,* and Fabrice Odobel**

Abstract: Dye-sensitized photocatalytic systems (DSPs) have been extensively investigated for solar-driven hydrogen (H_2) evolution. However, their application in carbon dioxide (CO_2) reduction remains limited. Furthermore, current solar-driven CO_2-to-CO DSPs typically employ rhenium complexes as catalysts. In this study, we have developed DSPs that incorporate noble metal-free components, specifically a zinc-porphyrin as photosensitizer (PS) and a cobalt-quaterpyridine as catalyst (CAT). Taking a significant stride forward, we have achieved an antenna effect for the first time in CO_2-to-CO DSPs by introducing a Bodipy as an additional chromophore to enhance light harvesting efficiency. The energy transfer from Bodipy to zinc porphyrin resulted in remarkable stability (turn over number (TON) = 759 vs. CAT), and high CO evolution activity (42 mmol g^{-1} h^{-1} vs. CAT).

Fossil fuels, such as natural gas, oil, and coal, constitute the universal primary energy sources.[1] Their prolonged and intensive usage gave rise to global warming and climate change.[2] Hence, there is an urgent need to establish a carbon-neutral and circular economy, by utilizing renewable energy sources to transform CO_2 into valuable fuels-chemicals.[3] Indeed, CO_2 can be converted into useful products, namely formic acid, carbon monoxide, methane, methanol, ethanol, and ethylene.[4] Even though the reduction of CO_2 into C_2^+ products (ethylene, ethanol, etc.) is of great commercial interest, carbon monoxide (CO) is also a valuable product of CO_2 reduction reaction (CO_2RR); since it can be obtained with high selectivity and yield.[5] Furthermore, CO production involves a $2e^-/2H^+$ process ($CO_2 + 2H^+ + 2e^- \rightarrow CO + H_2O$, $E^{o\prime} = -0.53$ V, vs. NHE, pH = 7) in contrast to ethanol and ethylene ($12e^-/12H^+$). In addition, CO is a multipurpose feedstock in numerous industrial applications.[3b,6]

Various strategies have been explored aiming at efficiently converting CO_2 into CO: i) electrocatalysis, ii) photocatalysis, ii) photoelectrocatalysis, iv) thermochemical, and v) biochemical conversion.[7] Among all the above-mentioned approaches, solar-driven CO_2-to-CO reduction stands out as an auspicious approach since the abundant, clean, and renewable solar energy is utilized directly without any other additional energy supply.[8] Over the last decades, numerous homogeneous, heterogeneous as well as hybrid systems combining molecular catalysts and solid/heterogeneous elements have been investigated,[9] including noble-metal free molecular systems in water as well.[10]

Dye-sensitized photocatalytic systems (DSPs) have great potential since they are extremely robust, highly tunable and potentially low-cost.[11] In a typical CO_2-to-CO reducing DSP system, nanoparticles (NPs) of a semiconductor (e.g. TiO_2) are functionalized with a photosensitizer (PS), and a CO_2R catalyst (CAT) in order to form the heterogeneous photocatalyst. Upon light excitation, the PS injects electrons to the conduction band (CB) of TiO_2, which are subsequently transferred to the CO_2R CAT. Finally, CO_2 is being reduced to CO, whereas the oxidized PS (PS^+) is regenerated by a sacrificial electron donor (SED). Interestingly, compared to the large number of DSPs for H_2 evolution in the literature,[11a,12] only a few CO_2 reducing DSPs have been developed, notably by S.O. Kang and co-workers.[13] However, in most of these examples, $ReCl(L)(CO)_3$ (L = 2,2′-bipyridine derivative) complex is the CO_2R CAT, containing one of the rarest elements in the earth's crust.[14] One example of noble metal-free DSP system for CO_2 photoreduction has been published, involving a Mn(I) catalyst for selective formate production (> 99 %) with a TON of 250.[15]

Herein, we present the first noble metal-free DSPs for CO_2-to-CO conversion, by utilizing a zinc-porphyrin (**ZnP**) as PS and a cobalt-quaterpyridine (**CoQPy**) as the CO_2R

[*] Dr. V. Nikolaou, Dr. S. Diring, Dr. F. Odobel
Nantes Université, CNRS, CEISAM, UMR 6230, F-44000 Nantes, France
E-mail: vasileios.nikolaou@univ-nantes.fr
fabrice.Odobel@univ-nantes.fr
Dr. C. Govind, Dr. E. Balanikas, Prof. Dr. E. Vauthey
Department of Physical Chemistry, University of Geneva, 30 Quai Ernest-Ansermet, CH-1211 Geneva, Switzerland
E-mail: eric.vauthey@unige.ch
J. Bharti, Prof. Dr. M. Robert
Laboratoire d'Electrochimie Moléculaire, Université Paris Cité, CNRS, F-75006 Paris, France
Prof. Dr. M. Robert
Institut Universitaire de France (IUF), F-75005, Paris, France
E-mail: robert@u-paris.fr

CAT. Moving one step forward, a Bodipy (**BDP**) was introduced as an additional light harvester to enhance photon capture. Thanks to energy transfer (EnT) from the **BDP** to the **ZnP**, antenna effect boosted the efficiency of DSP. Although this concept has been employed twice in DSPs for H_2 evolution,[16] a similar approach for CO_2-to-CO reduction has not yet been reported. As illustrated in Figure 1, the advantages of this photocatalytic systems are:

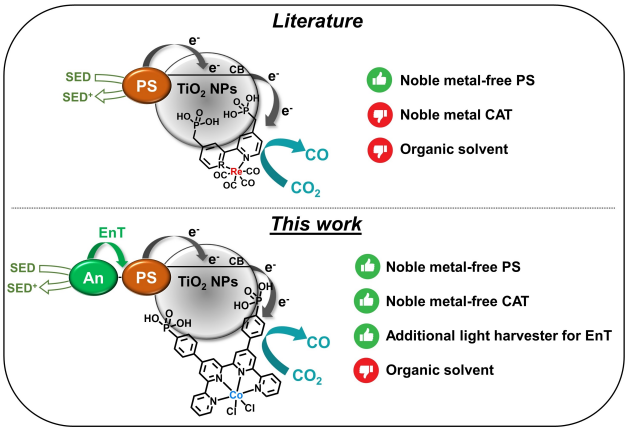

Figure 1. DSPs for CO_2-to-CO reduction: (upper panel) previous examples from literature; (lower panel) our strategy comprising a photo antenna component (An: BDP), a zinc porphyrin as sensitizer and a molecular cobalt catalyst.

i) the presence of a noble metal-free CAT and PS, and ii) the introduction of an additional chromophore (to enhance light harvesting efficiency and thereby the electron injection flux in TiO_2 nanoparticles) that may result in high efficiency for CO_2 reduction (in our case CO).

The preparations of Zinc-trimesitylporphyrin-benzoic acid (**ZnP**) and cobalt-quaterpyridine-bis phosphonic acid (**CoQPy**), were carried out following procedures reported in the literature, (Schemes S1–S2, Figures S1–S7).[16a,17] **ZnP** was selected as **PS**, not only because of its excellent properties in solar-harnessing application;[18] but also because this porphyrin is a very efficient TiO_2 sensitizer (in terms of electron injection)[19] and has been successfully tested as PS in homogeneous photocatalytic CO_2 and H^+ reduction systems.[18c,20] Concerning the CO_2 reduction part, we selected **CoQPy** as CAT,[17] because apart from being a noble metal-free catalyst, **CoQPy** has been shown to be a very efficient CO_2-to-CO reducing CAT in both homogeneous and heterogeneous systems.[9d,21] In addition, an imidazole-functionalized Bodipy (**BDP**)[22] was connected to ZnP through metallo-supramolecular interaction, aiming to augment the light collection and the photoexcitation rate of ZnP via an EnT process, thereby enhancing the catalytic activity.[23] In Scheme 1, the individual components of our DSPs, as well as the schematic representation of their preparation protocol are displayed (see ESI for experimental details). From absorption studies, atomic absorption, and infrared spectroscopy (IR) (Figure S8 and S9) the successful functionalization of TiO_2 surface was confirmed and the

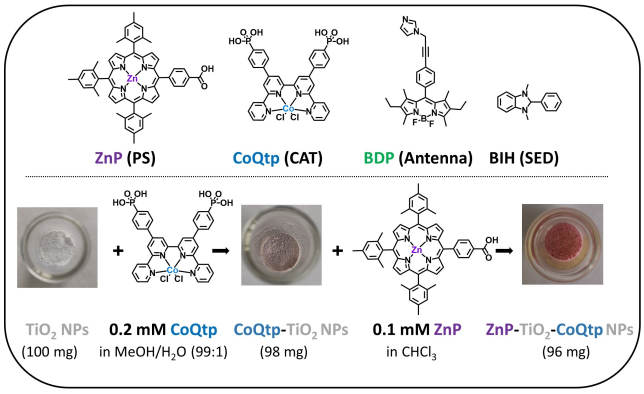

Scheme 1. Components (upper panel), and protocol used for the preparation of the DSPs (lower panel); All the experimental details are given in the ESI.

loading of **ZnP** and **CoQPy** was calculated (see ESI). In the final **ZnP-TiO_2-CoQPy** NPs, the **CoQPy** loading was 24 nmol/10 mg of TiO_2, while the **ZnP** amount was 0.22 μmol/10 mg of TiO_2, corresponding to the maximum loading in both cases.

The catalytic activity of our DSPs was evaluated by solar-driven CO_2 reduction measurements performed with LED light sources at different wavelengths. In a representative run, 10 mg of the ZnP-TiO_2-CoQPy NPs were dispersed in 4 mL of acetonitrile (ACN) solution containing the sacrificial electron donor (SED). The green-LED irradiation (525 nm) was the most efficient one as compared to the respective white and purple ones (see ESI and Figure S10), resulting in the production of 4.4 μmol of CO and 0.4 μmol of H_2 (92:8 ratio, entry 7 in Table 1).

We explored the impact of SED by testing triethanolamine (TEOA) and 1,3-Dimethyl-2-phenyl-2,3-dihydro-1H-benzo[d]imidazole (BIH), respectively. As illustrated in Table 1 (compare entries 7 and 9, Table 1), BIH was more efficient than TEOA leading to 11.0 μmol of CO and 3.6 μmol of H_2 (76:24 ratio). BIH is a stronger reductant than TEOA and can serve as a two-electron donor.[24] Upon adding water (entries 8 and 10, Table 1) the production of CO and H_2 decreased with both SEDs. This could be explained by the energy decrease of the TiO_2 CB, which diminishes the driving force to reduce **CoQPy**, as already demonstrated.[13a] Overall, the best results were obtained with BIH as SED and irradiation using a green-LED source (~525 nm). Control experiments showed no catalytic activity in the absence of any element of the system. From the data presented in Table 1, it is evident that neither CO nor H_2 was observed without: i) PS and CAT (entry 1), ii) PS (entry 2), iii) CAT (entry 3), iv) SED (entry 4), v) light Irradiation (entry 5), and vi) TiO_2 (entry 6). Transient absorption spectroscopy (TAS) measurements were performed (see below and additional details in the ESI) to shed some light on the photocatalytic mechanism in our DSPs.

Different amounts of BIH were used to determine the optimal concentration of the SED (Figure 2a). The CO vs. H_2 ratio remained nearly the same (~75:25) at all SED concentration. The maximum amount of product was

Table 1: Photocatalysis results under different conditions. All experiments were conducted using a green-LED lamp (~525 nm), except entry 14.

Entry	NPs	Solvent	SED	CO[a]	H_2[a]	CO/H_2
1	TiO_2	ACN	0.05 M BIH	ND[b]	ND	–
2	CoQPy-TiO_2	ACN	0.05 M BIH	ND	ND	–
3	ZnP-TiO_2	ACN	0.05 M BIH	ND	ND	–
4	ZnP-TiO_2-CoQPy	ACN	–	ND	ND	–
5[c]	ZnP-TiO_2-CoQPy	ACN	0.05 M BIH	ND	ND	–
6[d]	ZnP-CoQPy	ACN	0.05 M BIH	ND	ND	–
7	ZnP-TiO_2-CoQPy	ACN	0.1 M TEOA	4.4	0.4	92/8
8[e]	ZnP-TiO_2-CoQPy	ACN/H_2O	0.1 M TEOA	1.8	0.2	90/10
9	ZnP-TiO_2-CoQPy	ACN	0.05 M BIH	11.0	3.6	76/24
10[e]	ZnP-TiO_2-CoQPy	ACN/H_2O	0.05 M BIH	4.4	1.6	74/26
11	ZnP-TiO_2-CoQPy	ACN	0.025 M BIH	10.1	3.4	75/25
12	ZnP-TiO_2-CoQPy	ACN	0.1 M BIH	13.4	4.8	76/24
13	BDP-ZnP-TiO_2-CoQPy	ACN	0.1 M BIH	8.8	3.3	67/33
14[f]	BDP-ZnP-TiO_2-CoQPy	ACN	0.1 M BIH	18.2	9.3	66/34

[a] CO and H_2 quantities in μmol, upon reaching a production plateau. [b] ND: Not detected. [c] Without light irradiation. [d] Without TiO_2. [e] ACN + 3% H_2O. [f] Experiment performed using a white-LED lamp (400–700 nm).

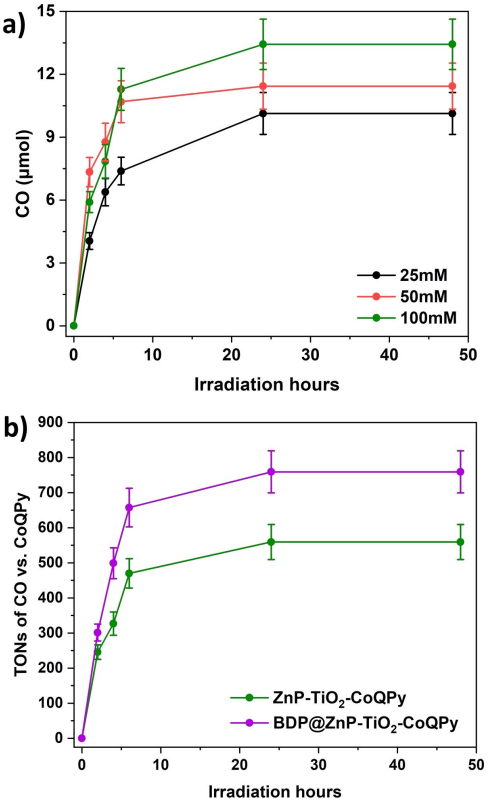

Figure 2. Photocatalytic CO_2-to-CO conversion activities of: a) ZnP-TiO_2-CoQPy DSPs (10 mg), in 4 mL of ACN solution with 25 mM (black), 50 mM (red), 100 mM (green) of BIH. b) ZnP-TiO_2-CoQPy (green line) versus BDP@ZnP-TiO_2-CoQPy DSPs (purple line). The reported CO quantities are the average of three independently repeated experiments.

obtained at 100 mM of SED, leading to the production of 13.4 μmol (CO) in 24 h of irradiation. Interestingly, by introducing **BDP** as a co-photosensitizer, the CO_2-to-CO production was significantly enhanced. Energy transfer (EnT) from Bodipy to ZnP is a well-established process, operating with an almost 100% quantum efficiency.[22,25] Remarkably, the CO evolution was significantly increased (from 13.4 to 18.2 μmol, compare entries 12 and 14 in Table 1), likely from the amplification of light harvesting efficiency. The BDP@ZnP-TiO_2-CoQPy DSPs were irradiated with two different light-sources, a green-LED (entry 13, Table 1) and a white-LED (entry 14, Table 1). Interestingly, the irradiation using the white-LED source led to higher-CO production. It may be ascribed to a better photon collection in the 450–550 nm window by **BDP**, before EnT to **ZnP** occurs. Indeed, **ZnP** exhibits an intense Soret band at 426 nm, and two Q-bands at 506 and 599 nm, whereas **BDP** has a sharp band at 526 nm (Figure S11) demonstrating complementary absorption features.[16a,26] The observed redshift regarding the Q-bands of **ZnP** demonstrates that **BDP** binds onto the **ZnP** through the imidazole unit. However, **BDP** may also bind onto TiO_2 surface via *H*-bonding between the imidazole and the proton of TiO_2,[16a,22] and possibly to the catalyst since cobalt loses its initial chloro ligands during catalysis (Figure S12).[27] Overall, BDP-ZnP-TiO_2-CoQPy DSPs demonstrated high stability (759 TONs vs. **CoQPy**) and CO activity (42 mmol g^{-1} h^{-1} vs. **CoQPy**), outperforming the respective ZnP-TiO_2-CoQPy DSPs which resulted in 558 TONs and 31 mmol g^{-1} h^{-1}, respectively.

Regardless of the different components (with/without **BDP**) and parameters (light source, amount of SED, etc.), deactivation of the system was observed after 24 h of irradiation. To elucidate the reason for this deactivation, a series of photocatalytic experiments were performed using ZnP-TiO_2-CoQPy DSPs (Figure S13). More precisely, after reaching a plateau for CO production (24 h), the DSP was relaunched by adding: a) **CoQPy**, b) **ZnP**, or c) **ZnP** + **CoQPy** respectively and by purging the suspension with CO_2. When **CoQPy** was added to the reaction vial (experiments a and c), the CO production was reactivated; whereas, by adding **ZnP** the system remained inactive. Consequently, the observed activity loss could most likely be attributed to **CoQPy**, which either leached from the TiO_2 NPs or was degraded; even though **CoQPy** has proven to be stable in

similar photocatalytic experiments.[21a] As anticipated, the CO production in the relaunched experiment c (**ZnP**+**CoQPy**) slightly surpassed the amount obtained in the experiment a (**CoQPy**), due to the additional light harvesting contribution by the new **ZnP** molecules. The origin of carbon in the produced CO was confirmed by conducting $^{13}CO_2$-labeled experiments. As shown in Figure S14, ^{13}CO was observed. It is worth mentioning that under N_2, no generation of carbon-containing product was observed. Collectively, all our results firmly demonstrate that the detected CO derives from CO_2.

To investigate the charge transfer dynamics of the photocatalytic system, we then carried out femtosecond transient absorption spectroscopy (fs TAS) measurements with **ZnP-TiO$_2$** and **ZnP-TiO$_2$-CoQPy** films, upon 550 nm photoexcitation (ZnP Q band). Such studies could reveal key parameters impacting the charge transfer dynamics between the PS, the CAT, and the TiO_2 NPs, and help elucidating the photocatalytic mechanism.[28] As illustrated in Figure 3a, the early TA spectra were dominated by

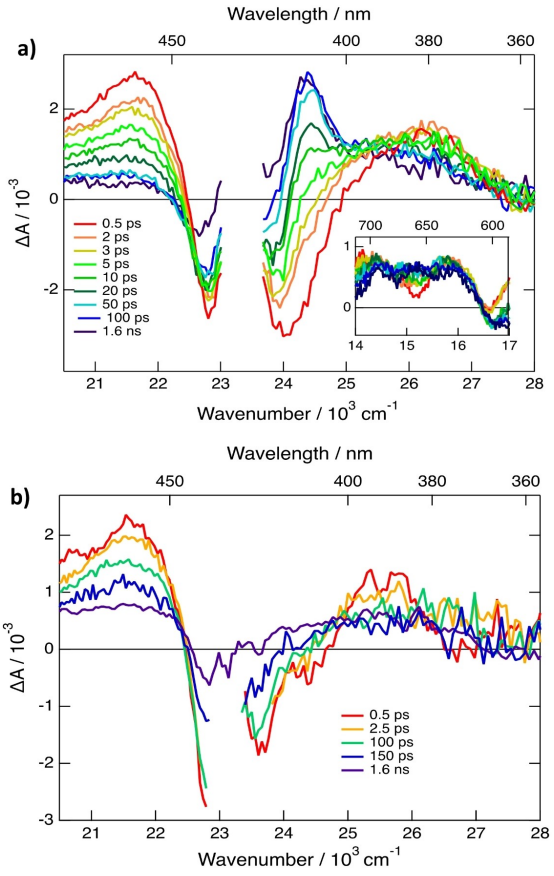

Figure 3. Transient absorption spectra recorded at various time delays after 550 nm excitation of ZnP-TiO_2 film without (**a**) and with 0.04 M BIH (**b**).

excited-state absorption (ESA) bands above 620 nm and around 460 nm and 380 nm, which can be assigned to the local S_1 state of the excited ZnP (PS*). Additionally, stimulated emission (SE) as well as ground-state bleach (GSB) features were visible at about 660 and 600 nm and in the 440–400 nm region.

Both the ESA and SE bands decayed in 11 ps, and a new band at 410 nm raised concurrently (Figure S15). This band can be assigned to the radical cation of the photosensitizer, $PS^{\bullet+}$, generated upon electron injection from PS* into TiO_2.[29] Charge injection into TiO_2 was further supported by mid-IR TAS measurements at 4000 nm, which showed the rise of the absorbance typical of electrons in the conduction band of TiO_2 (Figure S16).[30] The slower partial decay of the mid-IR absorbance can be attributed to charge recombination with $PS^{\bullet+}$.

In the presence of 0.04 M, the $PS^{\bullet+}$ band at 410 nm is hardly visible and the GSB was significantly reduced (Figure 3b). This difference can be attributed to a hole transfer from the radical cation of ZnP to BIH. The absence of the $PS^{\bullet+}$ band suggests that this hole transfer occurs on similar timescale as charge injection. As noted above, charge injection into TiO_2 was confirmed by mid-IR measurements. The decay of the TAS signal at 4000 nm was delayed in the presence of BIH. This effect is most probably due to the competition between hole transfer from $PS^{\bullet+}$ to BIH and charge recombination with the electron at the semiconductor surface. TA measurements with ZnP and 0.04 M BIH in acetonitrile indicated that reductive quenching of PS* by the SED is relatively inefficient and occurs with a rate constant well below the diffusion limit (Figures S17 and S18). Consequently, hole transfer from BIH to PS* is not competitive with electron injection into TiO_2. These two above-mentioned hole transfers are totally distinct processes. The first one is a hole transfer from $PS^{\bullet+}$ to BIH, whereas the second is a hole transfer from PS* to BIH. Both processes involve the oxidation of BIH, however the $PS^{\bullet+}$ is neutralized in the first one, while the PS* is reduced in the second one.

Finally, fs TA experiments with ZnP-TiO_2-CoQPy films in both the visible and the mid-IR pointed to the same dynamics as those found with ZnP-TiO_2 films (Figures S19 and S16). This suggests that electron transfer from TiO_2 to the catalyst is too slow to be observed within the time window of the experiment. In summary, the TA experiments suggest an oxidative quenching mechanism for the photocatalytic activity of our DSPs. In detail, photoexcitation of ZnP gives rise to the population of ZnP*, followed by ultrafast electron injection (11 ps) into TiO_2. The resulting $ZnP^{\bullet+}$ is rapidly regenerated by the SED ($ZnP^{\bullet+} \rightarrow ZnP$), whereas the electron diffuses in TiO_2 before being captured by the CoQPy. Given that two electrons (e^-) are required to reduce CO_2-to-CO, these above-mentioned processes should, in principle, occur twice to generate a CO molecule (Scheme 2).

In our study, we successfully achieved CO_2-to-CO DSPs by combining noble metal-free PS (**ZnP**) and CAT (**CoQPy**) derivatives. The incorporation of an additional chromophore (**BDP**) introduced an antenna effect, significantly enhancing CO photoproduction. Table 2 presents the TONs and CO production data for both previous systems reported in the literature and our novel approach. It is crucial to note that various parameters exert significant influence on the

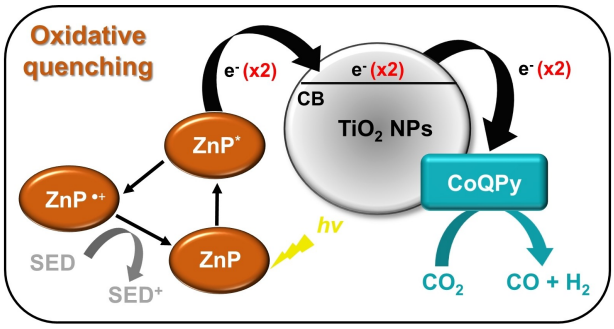

Scheme 2. Proposed photocatalytic mechanism for the two-electron reduction of CO_2 to CO in our DSPs.

Table 2: The TONs and the CO production rate of DSPs in the literature and in this work.

PS[a]	CAT[a]	TONs[b]	CO production[c]	Publication
2-H	Re-H	922	21.2	[13b]
SQ_{ca}	ReC	165	3.8	[31]
ZnP_{ca}	ReC	1028	39.4	[32]
Dye_1	ReP	180	29.0	[33]
MOD	RePH	570	–	[34]
Dye_2	ReC	435	–	[35]
BDP-ZnP	**CoQPy**	**759**	**42.1**	**this work**
ZnP	**CoQPy**	**559**	**31.0**	**this work**

[a] The molecular structures of all the different PSs and the CAT are shown in Figure S19. [b] TONs were calculated vs. CAT in all cases. [c] CO production is given in $mmol\,g^{-1}\,h^{-1}$ (g. of CAT). The CO production rates were calculated using the given data of each publication.

stability and production rate of such systems, including light intensity and source. In all prior reports, noble metal-free PSs were used in combination with $ReCl(L)(CO)_3$ (L = 2,2′-bipyridine derivative) as the CO_2R CAT. Molecular structures of all the different PSs and the Re-CAT can be found in Figure S20. Our work yielded promising results, with the highest recorded CO production rate reaching 42.1 $mmol\,g^{-1}\,h^{-1}$ (per g. of CAT), TONs amounting to 759, and an apparent quantum yield efficiency (AQY) of 3.9 % (see ESI). Building upon these encouraging findings, our ongoing research is now focusing on systems designed to operate in aqueous solutions without the need for sacrificial reagents—a crucial step towards the development of highly efficient CO_2 photocatalytic systems.

Supporting Information

Experimental details; synthesis and characterization; photocatalytic results; and transient absorption studies are provided. The authors have cited additional references within the Supporting Information.[36–39]

Acknowledgements

This project was supported by HORIZON TMA MSCA Postdoctoral Fellowships - European Fellowships (HORIZON-TMA-MSCA-PF-EF) action program under the call MSCA Postdoctoral Fellowships 2021 (HORIZON-MSCA-2021-PF-01) to V.N., grant agreement No. 101064765, SOLAR-CAT. This study also received financial support under the EUR LUMOMAT project and the Investments for the Future program ANR-18-EURE-0012. Financial support from the Swiss National Science Foundation (grant 200020-184607) and the University of Geneva is also acknowledged. Partial financial support to M.R. from the Institut Universitaire de France (IUF) is warmly thanked.

Conflict of Interest

The authors declare no conflict of interest.

Data Availability Statement

The data that support the findings of this study are available in the supplementary material of this article.

Keywords: CO_2 reduction · dye-sensitized photocatalytic systems (DSPs) · porphyrin · quaterpyridine · antenna effect

[1] J. L. Du, D. L. Xiang, K. X. Zhou, L. C. Wang, J. Y. Yu, H. H. Xia, L. L. Zhao, H. Liu, W. J. Zhou, *Nano Energy* **2022**, *104*, 107875.
[2] T. R. Knutson, R. Zhang, L. W. Horowitz, *Nat. Commun.* **2016**, *7*, 13676.
[3] a) M. Robert, *ACS Energy Lett.* **2016**, *1*, 281–282; b) J. C. Wood, Z. G. Yuan, B. Virdis, *Curr. Opin. Electrochem.* **2023**, *37*, 101177.
[4] Y. R. Lei, Z. Wang, A. Bao, X. L. Tang, X. B. Huang, H. H. Yi, S. Z. Zhao, T. Sun, J. Y. Wang, F. Y. Gao, *Chem. Eng. J.* **2023**, *453*, 139663.
[5] E. O. Eren, S. Ozkar, *J. Power Sources* **2021**, *506*, 230215.
[6] a) F. Zhang, Y. H. Li, M. Y. Qi, Y. M. A. Yamada, M. Anpo, Z. R. Tang, Y. J. Xu, *Chem. Catalysis* **2021**, *1*, 272–297; b) B. Cai, H. W. Cheo, T. Liu, J. Wu, *Angew. Chem. Int. Ed.* **2021**, *60*, 18950–18980.
[7] a) S. Amanullah, P. Saha, A. Nayek, M. E. Ahmed, A. Dey, *Chem. Soc. Rev.* **2021**, *50*, 3755–3823; b) Z. X. Bi, R. T. Guo, X. Hu, J. Wang, X. Chen, W. G. Pan, *Nanoscale* **2022**, *14*, 3367–3386; c) B. W. Deng, M. Huang, X. L. Zhao, S. Y. Mou, F. Dong, *ACS Catal.* **2022**, *12*, 331–362; d) X. J. Liu, T. Q. Chen, Y. H. Xue, J. C. Fan, S. L. Shen, M. S. A. A. Hossain, M. A. Amin, L. K. Pan, X. T. Xu, Y. Yamauchi, *Coord. Chem. Rev.* **2022**, *459*, 214440; e) S. Lu, F. L. Lou, Z. X. Yu, *Catalysts* **2022**, *12*, 228; f) A. Mustafa, B. G. Lougou, Y. Shuai, Z. J. Wang, H. P. Tan, *J. Energy Chem.* **2020**, *49*, 96–123; g) N. Nandal, S. L. Jain, *Coord. Chem. Rev.* **2022**, *451*, 214271; h) A. M. Parvez, M. T. Afzal, T. G. V. Hebb, M. Schmid, *J. CO2 Util.* **2020**, *40*, 101217; i) K. Torbensen, D. Joulie, S. X. Ren, M. Wang, D. Salvatore, C. P. Berlinguette, M. Robert, *ACS Energy Lett.* **2020**, *5*, 1512–1518; j) Q. S. Wang, Y. C. Yuan, C. F. Li, Z. R. Zhang, C. Xia, W. G. Pan, R. T. Guo, *Small* **2023**, *19*, 2301892; k) Y. W. Wang, D. He, H. Y. Chen, D. W.

Wang, *J. Photochem. Photobiol. C* **2019**, *40*, 117–149; l) Y. X. Zhou, D. D. Ma, J. W. Shi, *Cailiao Gongcheng* **2023**, *51*, 15–28.
[8] a) A. H. Behroozi, R. Xu, *Chem Catalysis* **2023**, *3*, 100550; b) A. Perazio, G. Lowe, R. Gobetto, J. Bonin, M. Robert, *Coord. Chem. Rev.* **2021**, *443*, 214018.
[9] a) M. Abdinejad, M. N. Hossain, H. B. Kraatz, *RSC Adv.* **2020**, *10*, 38013–38023; b) Y. H. Luo, L. Z. Dong, J. Liu, S. L. Li, Y. Q. Lan, *Coord. Chem. Rev.* **2019**, *390*, 86–126; c) D. Grammatico, A. J. Bagnall, L. Riccardi, M. Fontecave, B. L. Su, L. Billon, *Angew. Chem. Int. Ed.* **2022**, *61*, e2022063; d) A. Perazio, G. Lowe, R. Gobetto, J. Bonin, M. Robert, *Coord. Chem. Rev.* **2021**, *443*, 214018; e) C. Yang, S. Li, Z. Zhang, H. Wang, H. Liu, F. Jiao, Z. Guo, X. Zhang, W. Hu, *Small* **2020**, *16*, 2001847; f) P. De La Torre, L. An, C. J. Chang, *Adv. Mater.* **2023**, *35*, 2302122; g) N. Nandal, S. L. Jain, *Coord. Chem. Rev.* **2022**, *451*, 214271.
[10] a) X. Zhang, K. Yamauchi, K. Sakai, *ACS Catal.* **2021**, *11*, 10436–10449; b) F. Ma, Z.-M. Luo, J.-W. Wang, B. M. Aramburu-Trošelj, G. Ouyang, *Coord. Chem. Rev.* **2024**, *500*, 215529; c) A. Rosas-Hernández, C. Steinlechner, H. Junge, M. Beller, *Green Chem.* **2017**, *19*, 2356–2360.
[11] a) J. Willkomm, K. L. Orchard, A. Reynal, E. Pastor, J. R. Durrant, E. Reisner, *Chem. Soc. Rev.* **2016**, *45*, 9–23; b) G. Reginato, L. Zani, M. Calamante, A. Mordini, A. Dessi, *Eur. J. Inorg. Chem.* **2020**, *2020*, 899–917.
[12] a) L. Zani, M. Melchionna, T. Montini, P. Fornasiero, *J. Phys. Energy* **2021**, *3*, 031001; b) J.-F. Huang, Y. Lei, T. Luo, J.-M. Liu, *ChemSusChem* **2020**, *13*, 5863–5895.
[13] a) H. J. Son, C. Pac, S. O. Kang, *Acc. Chem. Res.* **2021**, *54*, 4530–4544; b) S. Choi, Y. J. Kim, S. Kim, H. S. Lee, J. Y. Shin, C. H. Kim, H. J. Son, S. O. Kang, *ACS Appl. Energ. Mater.* **2022**, *5*, 10526–10541; c) M. S. Choe, S. Choi, H. S. Lee, B. Chon, J. Y. Shin, C. H. Kim, H. J. Son, S. O. Kang, *ACS Appl. Mater. Interfaces* **2022**, *14*, 50718–50730.
[14] T. R. Crompton, in *Determination of Metals in Natural Waters, Sediments and Soils* (Ed.: T. R. Crompton), Elsevier, **2015**, pp. 161–178.
[15] S. J. Woo, S. Choi, S. Y. Kim, P. S. Kim, J. H. Jo, C. H. Kim, H. J. Son, C. Pac, S. O. Kang, *ACS Catal.* **2019**, *9*, 2580–2593.
[16] a) V. Nikolaou, G. Charalambidis, G. Landrou, E. Nikoloudakis, A. Planchat, R. Tsalameni, K. Junghans, A. Kahnt, F. Odobel, A. G. Coutsolelos, *ACS Appl. Energ. Mater.* **2021**, *4*, 10042–10049; b) P.-Y. Ho, M. F. Mark, Y. Wang, S.-C. Yiu, W.-H. Yu, C.-L. Ho, D. W. McCamant, R. Eisenberg, S. Huang, *ChemSusChem* **2018**, *11*, 2517–2528.
[17] P. B. Pati, R. Wang, E. Boutin, S. Diring, S. Jobic, N. Barreau, F. Odobel, M. Robert, *Nat. Commun.* **2020**, *11*, 3499.
[18] a) Y. Zhang, T. Higashino, H. Imahori, *J. Mater. Chem. A* **2023**, *11*, 12659–12680; b) D. Molina, J. Follana-Berná, Á. Sastre-Santos, *J. Mater. Chem. C* **2023**, *11*, 7885–7919; c) E. Nikoloudakis, I. López-Duarte, G. Charalambidis, K. Ladomenou, M. Ince, A. G. Coutsolelos, *Chem. Soc. Rev.* **2022**, *51*, 6965–7045.
[19] a) H. Imahori, S. Hayashi, T. Umeyama, S. Eu, A. Oguro, S. Kang, Y. Matano, T. Shishido, S. Ngamsinlapasathian, S. Yoshikawa, *Langmuir* **2006**, *22*, 11405–11411; b) M. Shrestha, L. Si, C.-W. Chang, H. He, A. Sykes, C.-Y. Lin, E. W.-G. Diau, *J. Phys. Chem. C* **2012**, *116*, 10451–10460; c) H. Hayashi, T. Higashino, Y. Kinjo, Y. Fujimori, K. Kurotobi, P. Chabera, V. Sundström, S. Isoda, H. Imahori, *ACS Appl. Mater. Interfaces* **2015**, *7*, 18689–18696; d) H. Imahori, S. Hayashi, H. Hayashi, A. Oguro, S. Eu, T. Umeyama, Y. Matano, *J. Phys. Chem. C* **2009**, *113*, 18406–18413; e) D. F. Watson, A. Marton, A. M. Stux, G. J. Meyer, *J. Phys. Chem. B* **2004**, *108*, 11680–11688; f) D. F. Watson, A. Marton, A. M. Stux, G. J. Meyer, *J. Phys. Chem. B* **2003**, *107*, 10971–10973; g) S. Hayashi, M. Tanaka, H. Hayashi, S. Eu, T. Umeyama, Y. Matano, Y. Araki, H. Imahori, *J. Phys. Chem. C* **2008**, *112*, 15576–15585; h) S. Ye, A. Kathiravan, H. Hayashi, Y. Tong, Y. Infahsaeng, P. Chabera, T. Pascher, A. P. Yartsev, S. Isoda, H. Imahori, V. Sundström, *J. Phys. Chem. C* **2013**, *117*, 6066–6080; i) R. Ide, Y. Fujimori, Y. Tsuji, T. Higashino, H. Imahori, H. Ishikawa, A. Imanishi, K.-i. Fukui, M. Nakamura, N. Hoshi, *ACS Omega* **2017**, *2*, 128–135.
[20] E. Agapaki, K. Ladomenou, V. Nikolaou, A. G. Coutsolelos, *J. Porphyrins Phthalocyanines* **2023**, *27*, 479–489.
[21] a) B. Ma, M. Blanco, L. Calvillo, L. Chen, G. Chen, T.-C. Lau, G. Dražić, J. Bonin, M. Robert, G. Granozzi, *J. Am. Chem. Soc.* **2021**, *143*, 8414–8425; b) P.-Y. Ho, S.-C. Cheng, F. Yu, Y.-Y. Yeung, W.-X. Ni, C.-C. Ko, C.-F. Leung, T.-C. Lau, M. Robert, *ACS Catal.* **2023**, *13*, 5979–5985; c) L. Chen, G. Chen, C.-F. Leung, C. Cometto, M. Robert, T.-C. Lau, *Chem. Soc. Rev.* **2020**, *49*, 7271–7283.
[22] J. Warnan, Y. Pellegrin, E. Blart, F. Odobel, *Chem. Commun.* **2012**, *48*, 675–677.
[23] B. Louahem M'Sabah, M. Boucharef, J. Warnan, Y. Pellegrin, E. Blart, B. Lucas, F. Odobel, J. Bouclé, *Phys. Chem. Chem. Phys.* **2015**, *17*, 9910–9918.
[24] Y. Pellegrin, F. Odobel, *C. R. Chim.* **2017**, *20*, 283–295.
[25] a) C. Y. Lee, J. T. Hupp, *Langmuir* **2010**, *26*, 3760–3765; b) M. J. Leonardi, M. R. Topka, P. H. Dinolfo, *Inorg. Chem.* **2012**, *51*, 13114–13122.
[26] E. Agapaki, K. Ladomenou, V. Nikolaou, A. G. Coutsolelos, *J. Porphyrins Phthalocyanines* **2023**, *27*, 479–489.
[27] M. Loipersberger, D. G. A. Cabral, D. B. K. Chu, M. Head-Gordon, *J. Am. Chem. Soc.* **2021**, *143*, 744–763.
[28] a) C. D. Windle, E. Pastor, A. Reynal, A. C. Whitwood, Y. Vaynzof, J. R. Durrant, R. N. Perutz, E. Reisner, *Chem. Eur. J.* **2015**, *21*, 3746–3754; b) A. Reynal, F. Lakadamyali, M. A. Gross, E. Reisner, J. R. Durrant, *Energy Environ. Sci.* **2013**, *6*, 3291–3300; c) M. Abdellah, A. M. El-Zohry, L. J. Antila, C. D. Windle, E. Reisner, L. Hammarström, *J. Am. Chem. Soc.* **2017**, *139*, 1226–1232.
[29] E. Nikoloudakis, P. B. Pati, G. Charalambidis, D. S. Budkina, S. Diring, A. Planchat, D. Jacquemin, E. Vauthey, A. G. Coutsolelos, F. Odobel, *ACS Catal.* **2021**, *11*, 12075–12086.
[30] A. Yamakata, T. Ishibashi, H. Onishi, *Chem. Phys. Lett.* **2001**, *333*, 271–277.
[31] M. Jo, S. Choi, J. H. Jo, S.-Y. Kim, P. S. Kim, C. H. Kim, H.-J. Son, C. Pac, S. O. Kang, *ACS Omega* **2019**, *4*, 14272–14283.
[32] D.-I. Won, J.-S. Lee, Q. Ba, Y.-J. Cho, H.-Y. Cheong, S. Choi, C. H. Kim, H.-J. Son, C. Pac, S. O. Kang, *ACS Catal.* **2018**, *8*, 1018–1030.
[33] J.-S. Lee, D.-I. Won, W.-J. Jung, H.-J. Son, C. Pac, S. O. Kang, *Angew. Chem. Int. Ed.* **2017**, *56*, 976–980.
[34] D.-I. Won, J.-S. Lee, J.-M. Ji, W.-J. Jung, H.-J. Son, C. Pac, S. O. Kang, *J. Am. Chem. Soc.* **2015**, *137*, 13679–13690.
[35] E.-G. Ha, J.-A. Chang, S.-M. Byun, C. Pac, D.-M. Jang, J. Park, S. O. Kang, *Chem. Commun.* **2014**, *50*, 4462–4464.
[36] J. S. Beckwith, A. Aster, E. Vauthey, *Phys. Chem. Chem. Phys.* **2022**, *24*, 568–577.
[37] B. Lang, S. Mosquera-Vazquez, D. Lovy, P. Sherin, V. Markovic, E. Vauthey, *Rev. Sci. Instrum.* **2013**, *84*, 073107–073108.
[38] M. Koch, R. Letrun, E. Vauthey, *J. Am. Chem. Soc.* **2014**, *136*, 4066–4074.
[39] S. Y. Fang, M. Rahaman, J. Bharti, E. Reisner, M. Robert, G. A. Ozin, Y. H. Hu, *Nat. Rev. Method Primers* **2023**, *3*, 61.

Manuscript received: November 29, 2023
Accepted manuscript online: February 5, 2024
Version of record online: ■■, ■■

Communications

CO_2 Reduction

V. Nikolaou,* C. Govind, E. Balanikas, J. Bharti, S. Diring, E. Vauthey,* M. Robert,* F. Odobel* _____ **e202318299**

Antenna Effect in Noble Metal-Free Dye-Sensitized Photocatalytic Systems Enhances CO_2-to-CO Conversion

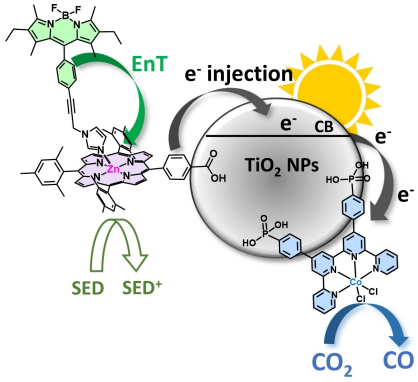

Efficient CO_2-to-CO dye-sensitized photocatalytic systems by utilizing noble metal-free photosensitizer (zinc-porphyrin) and catalyst (cobalt-quaterpyridine) derivatives. Upon introducing an additional chromophore (Bodipy), an antenna effect enhanced the photoproduction leading to 42.1 mmol g^{-1} h^{-1} of CO and 759 turn over numbers.